# Circularly Polarized Luminescence And Magneto-Optic Effect From a Chiral Dy(III)-Single-Molecule Magnet

Hong Huang,[a] Rong Sun,[b] Xiao-Fan Wu,[b] Youchao Liu,[a] Jun-Zheng Zhan,[a] Bing-Wu Wang,*[b] and Song Gao*[a,b]

a Spin-X Institute, School of Chemistry and Chemical Engineering, South China University of Technology, Guangzhou 510641, P. R. China.

b Beijing National Laboratory for Molecular Sciences, State Key Laboratory of Rare Earth Materials Chemistry and Applications, Beijing Key Laboratory for Magnetoelectric Materials and Devices, College of Chemistry and Molecular Engineering, Peking University, Beijing 100871, P. R. China.

E-mail: wangbw@pku.edu.cn; gaosong@scut.edu.cn

## Contents

## EXPERIMENTAL SECTION

### Syntheses:

All experiments were carried out under aerobic conditions. All the solvents in these experiments were analytical grade. The lanthanide nitrate salts were purchased from Energy Chemical. (*1R,2R*)-(+)-1,2-Diphenylethylenediamine and (*1S,2S*)-(-)-1,2-Diphenylethylenediamine were purchased from Energy Chemical.

The ligand Phenol, 2,2'-[[(*1S,2S*)-1,2-diphenyl-1,2-ethanediyl]bis[(E)-nitrilomethylidyne]]bis[6-methoxy or Phenol, 2,2'-[[(*1R,2R*)-1,2-diphenyl-1,2-ethanediyl]bis[(E)-nitrilomethylidyne]] have been synthesized according to a well-established procedure from the literature[1].

### Sample preparation

The stoichiometric reaction between 1*R, 2R*-$H_2L$ or 1*S, 2S*-$H_2L$ (0.25 mmol, 0.115 g), $Zn(OAc)_2 \cdot 2H_2O$ (0.25 mmol, 0.055 g) and $Dy(NO_3)_3 \cdot 6H_2O$ (0.3 mmol, 0.14 g) in 10 mL of Methanol gives a clear yellow solution. Heat to 75 °C overnight, slow diffusion of diethyl-ether yields to the formation of yellow crystals which are air stable over a period of several weeks. Yield = 65 % (based on Dy) 1R2R-$C_{30}H_{28}DyN_5O_{14}Zn$. Elemental analysis calcd. for 1R2R-$C_{30}H_{28}DyN_5O_{14}Zn$ (exp.): C 39.54 (39.33), H 3.07 (3.209), N 7.68 (7.38). Elemental analysis calcd. for 1S2S-$C_{30}H_{28}DyN_5O_{14}Zn$ (exp.): C 39.54 (39.38), H 3.07 (3.05), N 7.68 (7.58). IR (KBr, $cm^{-1}$) for 1R2R-$C_{30}H_{28}DyN_5O_{14}Zn$: 3621(w), 3476(w), 2931(w), 2841(w), 1634(s), 1466(s), 1386(m), 1281(m), 1213(m), 1084(w), 971(m), 738(s), 633(w), 542(w). IR (KBr, $cm^{-1}$) for 1S2S-$C_{30}H_{28}DyN_5O_{14}Zn$: 3621(w), 3476(w), 2931(w), 2841(w), 1634(s), 1466(s), 1386(m), 1281(m), 1213(m), 1084(w), 971(m), 738(s), 633(w), 542(w).

### Single-Crystal X-ray Diffraction Studies

Crystallographic data are presented in tables S1. The diffraction data were collected by using graphite-monochromatized Mo Kα radiation (λ = 0.71073 Å) at 150 K on an Agilent Bruker D8. The collection of the intensity data, cell refinement, and data

reduction were carried out with the program CrysAlisPro.[2] The structure was solved by the direct method with program SHELXS and refined with the least-squares program SHELXL.[3] Final refinements include anisotropic displacement parameters. The structure was verified using the ADDSYM algorithm from the program PLATON,[4] and no higher symmetry was found. Details of crystal parameters, data collection, and structure refinement are summarized in Table S1. The atomic coordinates and equivalent isotropic displacement parameters are listed in Table S2. The anisotropic displacement parameters are listed in Table S3, and the selected bond distances and angles are presented in Table S4.

**PXRD measurements.** Powder X-ray diffraction patterns (Figure S1) were measured on a Bruke D8 ADVANCE diffractometer using Cu-Ka radiation. The $2\theta$ range was 5-50 deg with a scan step width of 0.02 deg and a fixed counting time of 0.40 s/step.

**Elemental Analysis.** The C, H, and N microanalyses were carried out with a CE instruments EA 1110 elemental analyzer.

**FTIR measurements.** Fourier transform infrared (FTIR) spectra were obtained using a Bruker Tenor spectrophotometer.

**TGA measurements.** Thermogravimetric analysis (Figure S3a) was performed under nitrogen flow on a TGA-550 thermogravimetric analyzer. For 1R2R-ZnDy and 1S2S-ZnDy, TG analysis indicates that weight loss of 1.97 % occurred over the temperature range of 140 °C due to the loss of coordinated water molecules, and then the decompositions begin around 220 °C. obtained with a heating rate of 2 K/min.

**DSC measurements.** Differential scanning calorimetry (DSC) was performed using a Netzsch DSC 204 F1 at a heating speed of 2 K/min in a nitrogen gas atmosphere.

**CD measurements.** The CD data were obtained by Japanese JASCO company J-810 circular dichroic spectrometer (paired with JASCO 1.6 T permanent magnet accessories). The MCD spectra were measured using a JASCO J-810 equipped with a permanent magnet (+1.6 T or -1.6 T). The scanning wavelength range is from 200 nm to 600 nm at room temperature.

**UV measurements.** The absorption spectra were measured by the Jasco Corporation V-780 UV-Vis-NIR spectrophotometer. The scanning wavelength range is from 200 nm to 800 nm.

**Magnetic measurements.**

Samples were fixed by N-grease to avoid moving during measurement. Direct current susceptibility experiment was performed on Quantum Design MPMS XL-5 SQUID magnetometer on polycrystalline samples. Alternative current susceptibility measurements with frequencies ranging from 100 to 10000 Hz were performed on Quantum Design PPMS. All dc susceptibilities were corrected for diamagnetic contribution from the sample holder, N-grease and diamagnetic contributions from the molecule using the pascal's constants.

**CPL measurements.**

The circularly polarized luminescence (CPL) was measured on a Jasco CPL-300 spectrophotometer based on 'Continuous' scanning mode at 200 nm/min scan speed. The test mode adopts "Slit" mode with the Ex and Em Slit width 3000 μm and the digital integration time (D.I.T.) is 2.0 s with multiple accumulations (10 times or more).

**Theoretical analysis**

***Ab initio* calculation.** *Ab initio* calculations were performed at the CASSCF/SO-RASSI level of theory with the use of SINGLE_ANISO program [5-7] in MOLCAS 8.1 program[8]. Two models (**model 1** and **model 2**) were built based on the crystal

structures of two crystallographically independent molecules of 1R2R-ZnDy, respectively, and no further geometric optimization was conducted. The basis sets for all atoms are atomic natural orbitals from the MOLCAS ANO-RCC library[9-10]: ANO-RCC-VTZP for Dy(III) ions; VTZ for close N/O; VDZ for distant atoms. The calculations employed the second order Douglas-Kroll-Hess Hamiltonian, where scalar relativistic contractions were considered in the basis sets and the spin-orbit couplings were handled in the restricted active space state interaction (RASSI-SO) procedure. We have mixed the maximum number of spin-free states which was possible with our hardware (all from 21 sextets, 128 from 224 quadruplets, 130 from 490 doublets for the Dy(III) fragment). Active electrons in seven active spaces include all f electrons (CAS (9, 7)) of Dy (III) in the CASSCF calculation.

**DFT calculations.** Density functional theory (DFT) calculations were performed employing B3LYP functional [11-12] in Gaussian 09[13]. The calculated models were established on the basis of **model 1** and **model 2** by ulteriorly replacing Dy(III) with closed-shell Y(III). Then geometry optimization was performed and vibrational analysis were conducted. After that, time-dependent DFT (TD-DFT) were performed to help explore energy transitions. All calculations employed Stuttgardt–Dresden relativistic core potential (SDD) basis set for yttrium and 6-31G(d) basis set for the remaining elements with the solvent effect considered[14].

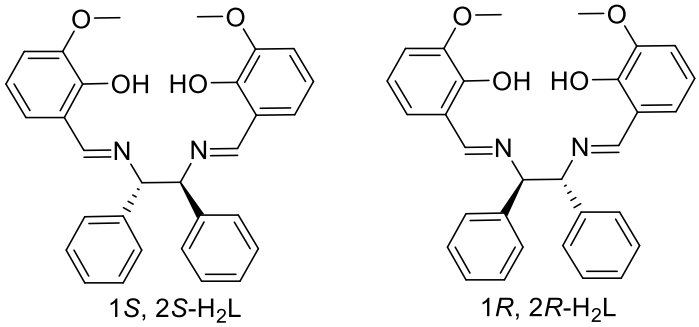


**Scheme S1.** Structure of the enantiopure 1*S,2S*-H2L and 1*R,2R*-H2L ligands.

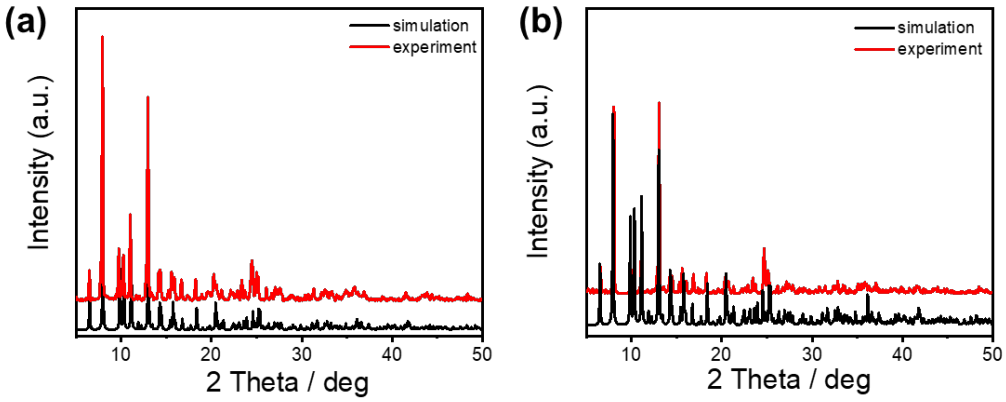


**Figure S1**. Powder X-ray diffraction pattern of 1R2R-ZnDy and 1S2S-ZnDy.

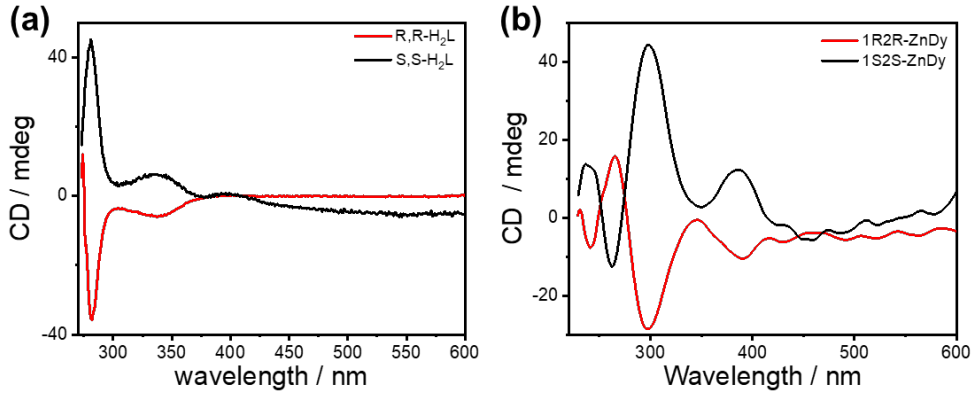


**Figure S2**. (a) CD spectra of Ligand in DMF (b) Room temperature solid-state CD spectra of 1R2R-ZnDy and 1S2S-ZnDy. recorded as KBr pellets.

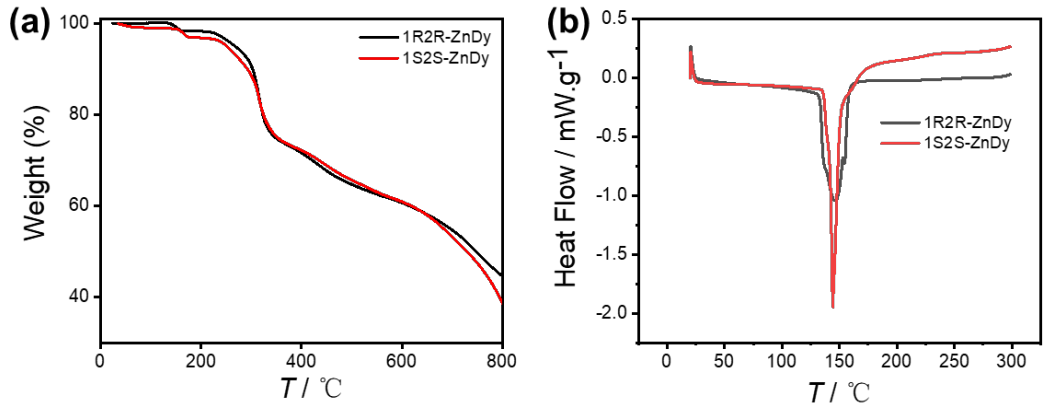


**Figure S3**. (a)TGA curves of 1R2R-ZnDy and 1S2S-ZnDy. (b) DSC curves of 1R2R-ZnDy and 1S2S-ZnDy.

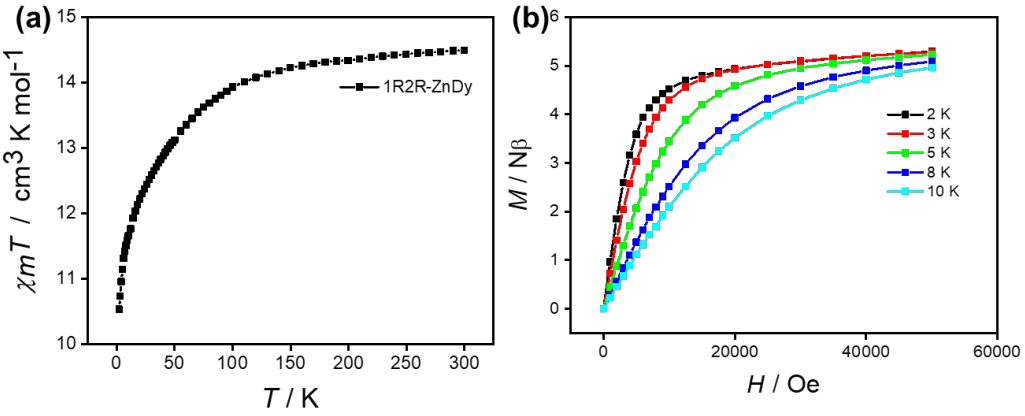


**Figure S4.** (a) Plots of temperature dependence of $\chi_M T$ for 1R2R-ZnDy under $H_{dc}$ = 1000 Oe between 2 and 300 K. (b) Magnetization versus H/T for compounds 1R2R-ZnDy.

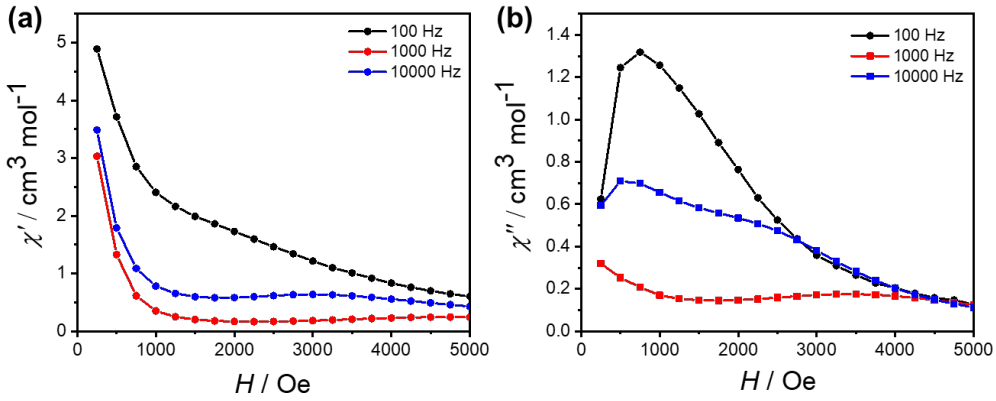


**Figure S5** Plots of field dependent in-phase (χ') and out-of-phase (χ″) component of ac susceptibility of 1R2R-ZnDy at 2 K

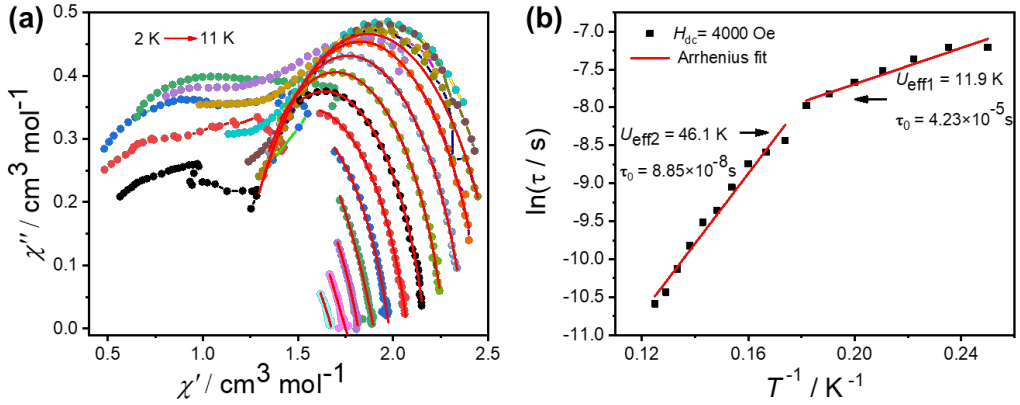


**Figure S6** (a) Cole-Cole plots for 1R2R-ZnDy obtained using the ac susceptibility data. The solid red lines correspond to the best fit obtained with a generalized Debye model.

(b) Temperature dependence of the relaxation time (τ). The solid red line is the best fit to the Arrhenius law.

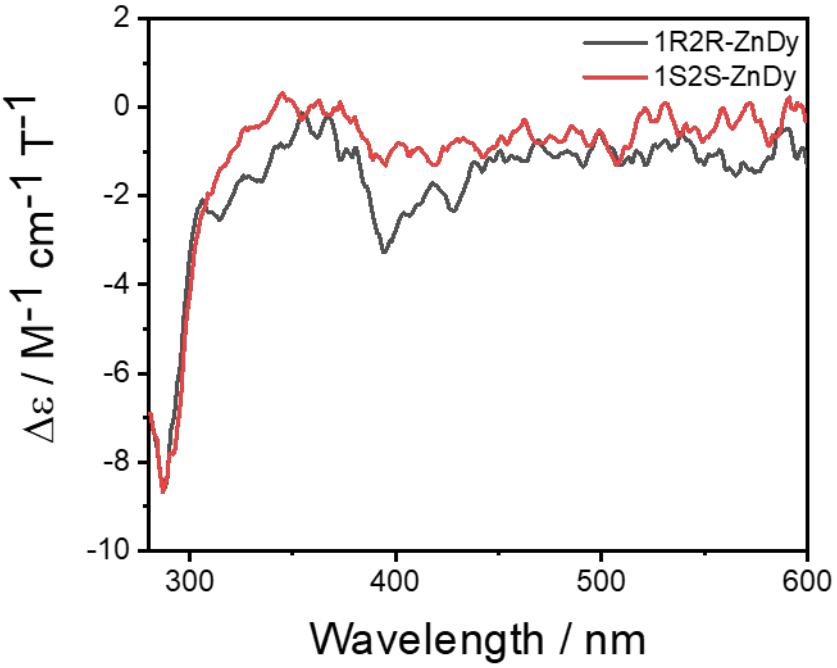


**Figure S7.** MCD spectra of 1R2R-ZnDy and 1S2S-ZnDy in DMF solution in the range of 280-600 nm at room temperature

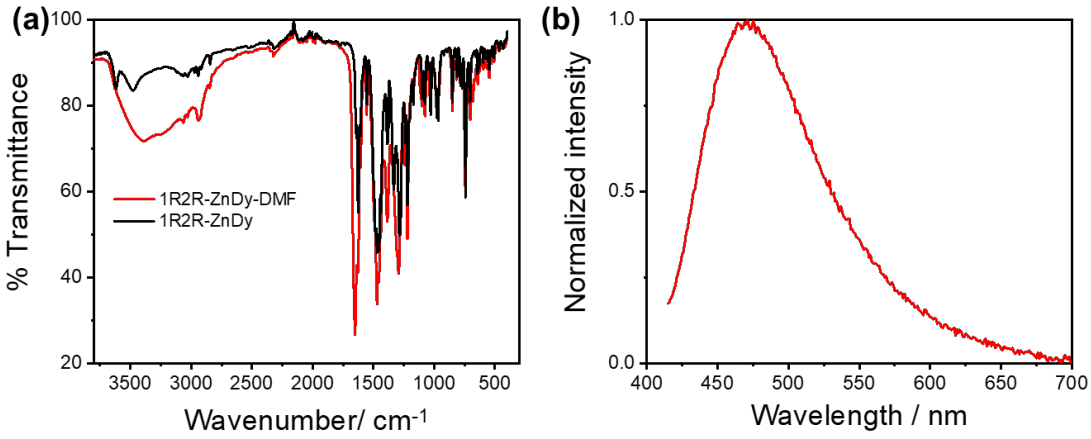


**Figure S8** (a) infrared spectrum (b) PL spectra of 1R2R-ZnDy in Toluene.

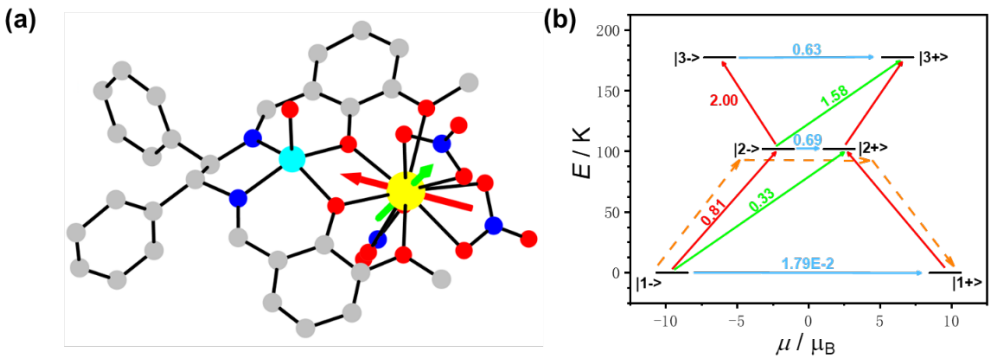


**Figure S9.** (a) Orientation of easy axes of the ground (red) and first-excited (green) Kramers doublets on **model 1** (Dy1B). (b) Magnetization reversal barrier of 1R2R-ZnDy. The thick black lines represent the Kramers doublets. The numbers at each arrow stand for the mean absolute value of the corresponding matrix element of the transition magnetic moment. The dashed orange arrows show the relaxation pathway.

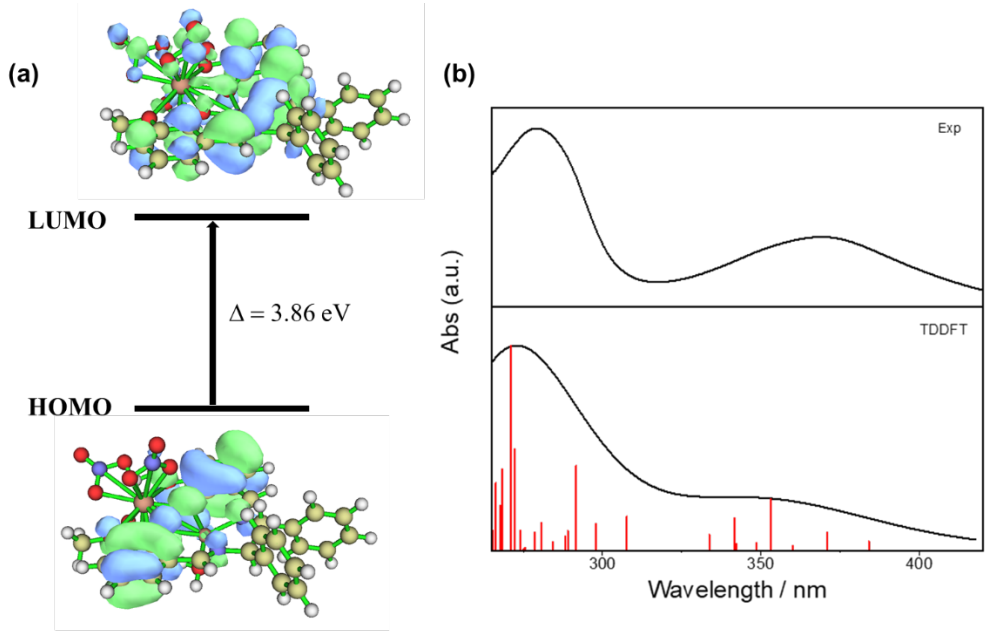


**Figure S10.** (a) HOMO LUMO of 1R2R-ZnDy. (b) Experimental (top) and TDDFT-predicted (bottom) UV-vis spectra of 1R2R-ZnDy complex using the B3LYP exchange-correlation functional.

**Table S1** Crystal data of **1S2S-ZnDy** and **1R2R-ZnDy**

| | **1S2S-ZnDy** | **1R2R-ZnDy** |
|---|---|---|
| Empirical formula | $C_{30}H_{28}DyN_5O_{14}Zn$ | $C_{30}H_{28}DyN_5O_{14}Zn$ |
| Formula weight | 910.44 | 910.44 |
| Temperature/K | 150.0 | 150.0 |
| Crystal system | Monoclinic | Monoclinic |
| Space group | $P2_1$ | $P2_1$ |
| a/Å | 9.0327(5) | 9.0362(6) |
| b/Å | 17.1436(7) | 17.1874(12) |
| c/Å | 22.4164(17) | 22.3670(14) |
| α/° | 90 | 90 |
| β/° | 97.007(5) | 97.150(2) |
| γ/° | 90 | 90 |
| Volume/Å$^3$ | 3445.3(4) | 3446.8(4) |
| Z | 4 | 4 |
| $\rho_{calc}$g/cm$^3$ | 1.755 | 1.754 |
| μ/mm$^{-1}$ | 2.923 | 2.922 |
| F(000) | 1804.0 | 1804.0 |
| Crystal size/mm$^3$ | 0.12 × 0.11 × 0.1 | 0.15 × 0.08 × 0.05 |
| Radiation | Mo Kα (λ = 0.71073) | Mo Kα (λ = 0.71073) |
| 2Θ range for data collection/° | 4.364 to 59.04 | 4.37 to 52.954 |
| Index ranges | $-10 \le h \le 11$, $-17 \le k \le 23$, $-31 \le l \le 25$ | $-10 \le h \le 11$, $-20 \le k \le 21$, $-27 \le l \le 28$ |
| Reflections collected | 20354 | 30139 |
| Independent reflections | 12822 [$R_{int}$ = 0.0399, $R_{sigma}$ = 0.0800] | 13003 [$R_{int}$= 0.1004, $R_{sigma}$ = 0.1315] |
| Data/restraints/parameters | 12822/82/926 | 13003/1355/925 |
| Goodness-of-fit on $F^2$ | 1.043 | 1.029 |
| Final R indexes [I>=2σ (I)] | $R_1$ = 0.0492, $wR_2$ = 0.0984 | R1 = 0.0610, wR2 = 0.1095 |

| | | |
|---|---|---|
| Final R indexes [all data] | $R_1$ = 0.0627, $wR_2$ = 0.1060 | R1 = 0.1273, wR2 = 0.1395 |
| Largest diff. peak/hole / e $Å^{-3}$ | 1.49/-1.25 | 0.92/-1.33 |
| Flack parameter | 0.008(18) | 0.03(2) |

**Table S2. Selected bond distances (Å) and angles (deg.) for 1R2R-ZnDy**.

| | | | |
|---|---|---|---|
| Dy2-O28 | 2.282(15) | Dy1- O12 | 2.45(2) |
| Dy2-O29 | 2.599(14) | Dy1- O2 | 2.352(16) |
| Dy2-O27 | 2.322(16) | Dy1- O1 | 2.310(14) |
| Dy2-O16 | 2.438(19) | Dy1- O11 | 2.613(17) |
| Dy2-O23 | 2.47(2) | Dy1- O9 | 2.48(2) |
| Dy2- N6 | 2.83(3) | Dy1- O13 | 2.42(2) |
| Dy2- O21 | 2.676(17) | Dy1- O5 | 2.462(18) |
| Dy2- O19 | 2.570(19) | Dy1- O4 | 2.582(15) |
| Dy2- N8 | 2.90(3) | Dy1- N5 | 2.85(2) |
| Dy2-O18 | 2.473(18) | Dy1- O8 | 2.46(2) |
| Dy2-O17 | 2.39(2) | Dy1- O6 | 2.61(2) |
| Dy2-O24 | 2.43(2) | Dy1- N3 | 2.89(3) |
| Zn2-O28 | 2.007(16) | Zn1- O2 | 1.971(15) |
| Zn2-O27 | 1.993(16) | Zn1- O1 | 1.996(15) |
| Zn2-N10 | 1.97(2) | Zn1- O3 | 2.032(17) |
| Zn2-O26 | 2.00(2) | Zn1- N2 | 2.046(18) |
| Zn2-N9 | 2.076(18) | Zn1- N1 | 2.05(2) |
| O28-Dy2- O29 | 129.3(5) | O12-Dy1-O11 | 127.3(5) |
| O28-Dy2- O27 | 67.0(5) | O12-Dy1-O9 | 141.8(6) |
| O28-Dy2- O16 | 76.2(6) | O12-Dy1-O5 | 72.9(7) |
| O28-Dy2- O23 | 79.9(7) | O12-Dy1-O4 | 77.3(5) |
| O28-Dy2- N6 | 79.6(7) | O12-Dy1-N5 | 26.5(5) |
| O28-Dy2- O21 | 60.4(6) | O12-Dy1-O8 | 148.6(6) |

| | | | |
|---|---|---|---|
| O28-Dy2- O19 | 117.7(6) | O12-Dy1-O6 | 106.9(7) |
| O28-Dy2-N8 | 104.0(8) | O12-Dy1-N3 | 154.8(5) |
| O28-Dy2- O18 | 149.0(6) | O2-Dy1-O12 | 71.2(6) |
| O28-Dy2- O17 | 87.3(7) | O2-Dy1-O11 | 122.3(5) |
| O28- Dy2- O24 | 129.2(8) | O2-Dy1-O9 | 111.8(6) |
| O29- Dy2-N6 | 102.1(7) | O2-Dy1-O13 | 112.6(7) |
| O29-Dy2-O21 | 155.3(6) | O2-Dy1-O5 | 124.3(6) |
| O29-Dy2-N8 | 77.9(7) | O2-Dy1-O4 | 62.0(5) |
| O27-Dy2-O29 | 62.3(5) | O2-Dy1-N5 | 90.8(6) |
| O27-Dy2-O16 | 112.5(7) | O2-Dy1-O8 | 77.4(7) |
| O27-Dy2-O23 | 77.2(7) | O2-Dy1-O6 | 173.9(6) |
| O27-Dy2-N6 | 90.9(7) | O2-Dy1-N3 | 94.8(7) |
| O27-Dy2-O21 | 121.8(6) | O1-Dy1-O12 | 87.8(6) |
| O27 -Dy2-O19 | 174.5(6) | O1-Dy1-O2 | 65.8(5) |
| O27 -Dy2-N8 | 93.0(8) | O1-Dy1-O11 | 62.0(6) |
| O27-Dy2-O18 | 124.1(6) | O1-Dy1-O9 | 129.1(7) |
| O27-Dy2-O17 | 71.0(7) | O1-Dy1-O13 | 75.9(6) |
| O27-Dy2-O24 | 109.8(7) | O1-Dy1-O5 | 151.1(6) |
| O16-Dy2-O29 | 124.7(6) | O1-Dy1-O4 | 127.7(5) |
| O16- Dy2-O23 | 147.3(6) | O1-Dy1-N5 | 79.5(6) |
| O16- Dy2-N6 | 26.3(6) | O1-Dy1-O8 | 80.4(6) |
| O16- Dy2-O21 | 77.9(6) | O1-Dy1-O6 | 120.2(6) |
| O16- Dy2-O19 | 67.2(7) | O1-Dy1-N3 | 105.8(7) |
| O16- Dy2-N8 | 151.4(7) | O11-Dy1-N5 | 101.9(6) |
| O16- Dy2-O18 | 73.0(6) | O11-Dy1-N3 | 77.9(6) |
| O23- Dy2-O29 | 87.7(6) | O9-Dy1-O11 | 84.8(6) |
| O23- Dy2- N6 | 159.0(7) | O9-Dy1-O4 | 72.1(6) |
| O23- Dy2- O21 | 71.0(6) | O9-Dy1-N5 | 148.5(6) |
| O23- Dy2- O19 | 106.1(7) | O9-Dy1-O6 | 65.9(7) |

| | | | |
|---|---|---|---|
| O23- Dy2- N8 | 25.1(7) | O9-Dy1-N3 | 25.2(6) |
| O23- Dy2- O18 | 129.1(7) | O13-Dy1-O12 | 53.6(6) |
| N6- Dy2- N8 | 175.5(8) | O13-Dy1-O11 | 76.6(6) |
| O21- Dy2- N6 | 102.1(6) | O13-Dy1-O9 | 135.2(7) |
| O21- Dy2- N8 | 77.6(7) | O13-Dy1-O5 | 75.3(6) |
| O19- Dy2- O29 | 113.0(6) | O13-Dy1-O4 | 126.1(6) |
| O19- Dy2- N6 | 87.2(8) | O13-Dy1-N5 | 27.2(6) |
| O19- Dy2- O21 | 63.7(6) | O13-Dy1-O8 | 146.7(6) |
| O19- Dy2- N8 | 88.7(8) | O13-Dy1-O6 | 69.3(7) |
| O18- Dy2- O29 | 69.9(5) | O13-Dy1-N3 | 149.6(7) |
| O18- Dy2- N6 | 71.9(7) | O5-Dy1-O11 | 113.2(6) |
| O18- Dy2- O21 | 113.9(6) | O5-Dy1-O9 | 75.4(7) |
| O18- Dy2- O19 | 50.4(6) | O5-Dy1-O4 | 69.7(6) |
| O18- Dy2- N8 | 104.0(8) | O5-Dy1-N5 | 73.6(6) |
| O17- Dy2- O29 | 78.0(6) | O5-Dy1-O6 | 50.0(7) |
| O17- Dy2- O16 | 52.3(6) | O5-Dy1-N3 | 100.4(7) |
| O17- Dy2- O23 | 148.1(7) | O4-Dy1-O11 | 155.4(6) |
| O17- Dy2- N6 | 26.1(6) | O4-Dy1-N5 | 102.2(6) |
| O17- Dy2- O21 | 126.7(6) | O4-Dy1-O6 | 112.1(6) |
| O17- Dy2- O19 | 105.7(7) | O4-Dy1-N3 | 77.6(6) |
| O17- Dy2- N8 | 155.2(6) | N5-Dy1-N3 | 173.5(6) |
| O17- Dy2- O18 | 72.3(7) | O8-Dy1-O11 | 71.7(6) |
| O17- Dy2- O24 | 141.9(7) | O8-Dy1-O9 | 51.8(6) |
| O24- Dy2- O29 | 70.2(7) | O8-Dy1-O5 | 126.8(7) |
| O24- Dy2- O16 | 137.0(8) | O8-Dy1-O4 | 87.0(6) |
| O24- Dy2- O23 | 51.8(8) | O8-Dy1-N5 | 159.5(6) |
| O24- Dy2- N6 | 149.0(8) | O8-Dy1-O6 | 104.2(7) |
| O24- Dy2- O21 | 86.6(7) | O8-Dy1-N3 | 26.6(6) |
| O24- Dy2- O19 | 69.9(8) | O6-Dy1-O11 | 63.6(6) |

| | | | |
|---|---|---|---|
| O24- Dy2- N8 | 26.7(7) | O6-Dy1-N5 | 89.3(7) |
| O24- Dy2- O18 | 77.4(8) | O6-Dy1-N3 | 84.8(7) |
| O28-Zn2-Dy2 | 39.0(4) | O2-Zn1-Dy1 | 40.2(5) |
| O28-Zn2-N9 | 88.3(7) | O2-Zn1-O1 | 79.3(6) |
| O27-Zn2-Dy2 | 40.0(4) | O2-Zn1-O3 | 98.3(7) |
| O27-Zn2-O28 | 78.9(6) | O2-Zn1-N2 | 152.8(8) |
| O27-Zn2-O26 | 105.8(8) | O2-Zn1-N1 | 92.3(8) |
| O27-Zn2-N9 | 145.5(8) | O1-Zn1-Dy1 | 39.2(4) |
| N10-Zn2-Dy2 | 128.6(6) | O1-Zn1-O3 | 108.6(8) |
| N10-Zn2-O28 | 149.1(9) | O1-Zn1-N2 | 88.8(6) |
| N10-Zn2-O27 | 93.6(7) | O1-Zn1-N1 | 143.4(9) |
| N10-Zn2-O26 | 106.8(8) | O3-Zn1-Dy1 | 105.7(6) |
| N10-Zn2-N9 | 81.1(8) | O3-Zn1-N2 | 108.7(8) |
| O26-Zn2-Dy2 | 107.0(6) | O3-Zn1-N1 | 107.8(8) |
| O26-Zn2-O28 | 104.0(8) | N2-Zn1-Dy1 | 124.8(5) |
| O26-Zn2-N9 | 108.3(8) | N2-Zn1-N1 | 82.7(8) |
| N9-Zn2-Dy2 | 122.1(5) | N1-Zn1-Dy1 | 124.9(6) |

**Table S3. Selected bond distances (Å) and angles (deg.) for 1S2S-ZnDy.**

| | | | |
|---|---|---|---|
| Dy1-N3 | 2.901(12) | Dy2- O24 | 2.529(10) |
| Dy1- O3 | 2.463(10) | Dy2- O19 | 2.449(9) |
| Dy1- O00X | 2.601(8) | Dy2- N8 | 2.840(11) |
| Dy1- O8 | 2.621(10) | Dy2- N10 | 2.885(13) |
| Dy1- O9 | 2.462(9) | Zn1- O5 | 2.016(7) |
| Dy1- O12 | 2.434(11) | Zn-O6 | 2.004(8) |
| Dy1- O2 | 2.494(11) | Zn1- N2 | 2.018(11) |
| Dy2- O17 | 2.407(12) | Zn1- O14 | 2.014(9) |
| Dy2- O16 | 2.583(8) | Zn1- N1 | 2.048(9) |

| | | | |
|---|---|---|---|
| Dy2- O21 | 2.675(8) | Zn2- O00C | 2.009(9) |
| Dy2- O00C | 2.289(8) | Zn2- O15 | 1.978(8) |
| Dy2- O27 | 2.462(10) | Zn2- O4 | 1.997(9) |
| Dy2- O15 | 2.360(9) | Zn2- N7 | 2.055(9) |
| Dy2- O26 | 2.486(10) | Zn2- N6 | 2.010(11) |
| Dy2- O22 | 2.485(9) | O17-Dy2-O16 | 78.0(3) |
| O5-Dy1-O11 | 112.1(3) | O17-Dy2-O21 | 127.0(3) |
| O5-Dy1-O7 | 123.0(3) | O17-Dy2-O27 | 141.6(3) |
| O5-Dy1-N5 | 90.4(3) | O17-Dy2--O26 | 147.8(3) |
| O5-Dy1-N3 | 94.7(3) | O17-Dy2-O22 | 73.5(3) |
| O5-Dy1-O3 | 79.2(3) | O17-Dy2-O24 | 106.7(3) |
| O5-Dy1-O00X | 61.5(3) | O17-Dy2-O19 | 53.0(3) |
| O5-Dy1-O8 | 173.1(3) | O17-Dy2-N8 | 26.1(3) |
| O5-Dy1-O9 | 122.7(3) | O17-Dy2-N10 | 154.7(3) |
| O5-Dy1-O12 | 70.7(3) | O16-Dy2-O21 | 155.1(3) |
| O5-Dy1-O2 | 111.2(3) | O16-Dy2-N8 | 102.1(3) |
| O6-Dy1-O5 | 66.4(2) | O16-Dy2-N10 | 76.9(3) |
| O6-Dy1-O11 | 75.7(3) | O21-Dy2-N8 | 102.5(3) |
| O6-Dy1-O7 | 62.1(3) | O21-Dy2-N10 | 78.2(3) |
| O6-Dy1-N5 | 79.2(3) | O00C-Dy2-O17 | 86.7(3) |
| O6-Dy1-N3 | 106.4(3) | O00C-Dy2-O16 | 128.4(3) |
| O6-Dy1-O3 | 81.5(3) | O00C-Dy2-O21 | 60.9(3) |
| O6-Dy1-O00X | 127.9(3) | O00C-Dy2-O27 | 130.4(4) |
| O6-Dy1-O8 | 120.2(3) | O00C-Dy2-O15 | 66.2(3) |
| O6-Dy1-O9 | 150.6(3) | O00C-Dy2-O26 | 81.2(3) |
| O6-Dy1-O12 | 87.2(3) | O00C-Dy2-O22 | 149.3(3) |
| O6-Dy1-O2 | 130.4(3) | O00C-Dy2-O24 | 117.4(3) |
| O11-Dy1-O7 | 77.2(3) | O00C-Dy2-O19 | 76.2(3) |
| O11-Dy1-N5 | 26.7(3) | O00C-Dy2-N8 | 79.3(3) |

| | | | |
|---|---|---|---|
| O11-Dy1-N3 | 150.7(3) | O00C-Dy2-N10 | 106.3(4) |
| O11-Dy1-O3 | 146.9(3) | O27-Dy2-O16 | 70.8(3) |
| O11-Dy1-O00X | 125.6(3) | O27-Dy2-O21 | 86.2(3) |
| O11-Dy1-O8 | 69.5(3) | O27-Dy2-O26 | 52.1(4) |
| O11-Dy1-O9 | 75.2(3) | O27-Dy2-O22 | 75.6(3) |
| O11-Dy1-O12 | 52.7(3) | O27-Dy2-O24 | 68.4(4) |
| O11-Dy1-O2 | 136.0(4) | O27-Dy2-N8 | 147.8(4) |
| O7-Dy1-N5 | 102.0(3) | O27-Dy2-N10 | 25.9(4) |
| O7-Dy1-N3 | 78.4(3) | O15-Dy2-O17 | 70.6(3) |
| O7-Dy1-O00X | 155.3(3) | O15-Dy2-O16 | 62.2(3) |
| O7-Dy1-O8 | 63.8(3) | O15-Dy2-O21 | 121.3(3) |
| N5-Dy1-N3 | 173.6(3) | O15-Dy2-O27 | 111.4(3) |
| O3-Dy1-O7 | 71.0(3) | O15-Dy2-O26 | 77.2(4) |
| O3-Dy1-N5 | 160.4(3) | O15-Dy2-O22 | 125.1(3) |
| O3-Dy1-N3 | 25.6(3) | O15-Dy2-O24 | 175.7(3) |
| O3-Dy1-O00X | 87.3(3) | O15-Dy2-O19 | 112.7(3) |
| O3-Dy1-O8 | 103.2(3) | O15-Dy2-N8 | 90.6(3) |
| O3-Dy1-O2 | 51.2(4) | O15-Dy2-N10 | 94.4(4) |
| O00X-Dy1-N5 | 102.3(3) | O26-Dy2-O16 | 86.4(3) |
| O00X-Dy1-N3 | 77.0(3) | O26-Dy2-O21 | 71.6(3) |
| O00X-Dy1-O8 | 111.9(3) | O26-Dy2-O24 | 105.4(4) |
| O8-Dy1-N5 | 89.1(3) | O26-Dy2-N8 | 160.0(3) |
| O8-Dy1-N3 | 85.3(3) | O26-Dy2-N10 | 26.2(4) |
| O9-Dy1-O7 | 114.1(3) | O22-Dy2-O16 | 70.9(3) |
| O9-Dy1-N5 | 73.2(3) | O22-Dy2-O21 | 113.3(3) |
| O9-Dy1-N3 | 100.8(3) | O22-Dy2-O26 | 127.4(3) |
| O9-Dy1-O3 | 126.3(3) | O22-Dy2-O24 | 50.5(3) |
| O9-Dy1-O00X | 69.0(3) | O22-Dy2-N8 | 72.6(3) |
| O9-Dy1-O8 | 50.7(3) | O22-Dy2-N10 | 101.3(4) |

| | | | |
|---|---|---|---|
| O9-Dy1-O2 | 75.3(3) | O24-Dy2-O16 | 114.2(3) |
| O12-Dy1-O7 | 127.0(3) | O24-Dy2-O21 | 63.0(3) |
| O12-Dy1-N5 | 26.2(3) | O24-Dy2-N8 | 87.8(3) |
| O12-Dy1-N3 | 154.6(3) | O24-Dy2-N10 | 86.9(4) |
| O12-Dy1-O3 | 149.8(3) | O19-Dy2-O16 | 125.4(3) |
| O12-Dy1-O00X | 77.7(3) | O19-Dy2-O21 | 77.7(3) |
| O12-Dy1-O8 | 106.7(3) | O19-Dy2-O27 | 135.2(3) |
| O12-Dy1-O9 | 72.4(3) | O19-Dy2-O26 | 148.1(3) |
| O12-Dy1-O2 | 141.0(3) | O19-Dy2-O22 | 73.2(3) |
| O2-Dy1-O7 | 86.0(3) | O19-Dy2-O24 | 66.9(3) |
| O2-Dy1-N5 | 148.1(3) | O19-Dy2-N8 | 27.0(3) |
| O2-Dy1-N3 | 25.6(3) | O19-Dy2-N10 | 150.4(3) |
| O2-Dy1-O00X | 70.8(3) | N8-Dy2-N10 | 173.6(4) |
| O2-Dy1-O8 | 66.6(4) | O00C-Zn2-Dy2 | 38.7(2) |
| O5-Zn1-Dy1 | 39.6(2) | O00C-Zn2-N7 | 88.0(4) |
| O5-Zn1-N2 | 92.5(4) | O00C-Zn2-N6 | 149.8(4) |
| O5-Zn1-N1 | 152.7(4) | O15-Zn2-Dy2 | 40.5(2) |
| O6-Zn1-Dy1 | 39.00(19) | O15-Zn2-O00C | 79.1(3) |
| O6-Zn1-O5 | 78.5(3) | O15-Zn2-O4 | 104.8(4) |
| O6-Zn1-N2 | 140.5(4) | O15-Zn2-N7 | 145.4(4) |
| O6-Zn1-O14 | 111.1(4) | O15-Zn2-N6 | 92.2(4) |
| O6-Zn1-N1 | 88.6(3) | O4-Zn2-Dy2 | 106.6(3) |
| N2-Zn1-Dy1 | 123.8(3) | O4-Zn2-O00C | 103.9(4) |
| N2-Zn1-N1 | 82.3(4) | O4-Zn2-N7 | 109.4(4) |
| O14-Zn1-Dy1 | 107.0(3) | O4-Zn2-N6 | 106.3(4) |
| O14-Zn1-O5 | 98.8(4) | N7-Zn2-Dy2 | 121.3(3) |
| O14-Zn1-N2 | 108.2(4) | N6-Zn2-Dy2 | 127.9(3) |
| O14-Zn1-N1 | 108.3(4) | N6-Zn2-N7 | 83.0(4) |
| N1-Zn1-Dy1 | 124.8(3) | | |

**Table S4. Calculated energy levels and *g* ($g_x$, $g_y$, $g_z$) tensors of the lowest Kramers doublets (KDs) of individual Dy(III) fragment for model 1(Dy1A) and model 1(Dy1B) for 1R2R-ZnDy.**

| KDs | 1 | | | 2 | | |
|---|---|---|---|---|---|---|
| | *E* / $cm^{-1}$ | *E* / K | *g* | *E* / $cm^{-1}$ | *E* / K | *g* |
| 1 | 0.0 | 0.0 | 0.041<br>0.049<br>18.888 | 0.0 | 0.0 | 0.038<br>0.070<br>19.116 |
| 2 | 68.9 | 99.0 | 0.910<br>2.350<br>17.189 | 70.9 | 101.9 | 0.818<br>2.586<br>17.238 |
| 3 | 98.4 | 141.5 | 0.536<br>1.280<br>17.147 | 123.4 | 177.5 | 0.015<br>2.443<br>14.092 |
| 4 | 131.4 | 188.9 | 0.319<br>3.229<br>10.869 | 153.3 | 220.4 | 0.182<br>1.249<br>14.949 |
| 5 | 185.8 | 267.2 | 0.407<br>2.445<br>13.678 | 179.6 | 258.2 | 0.795<br>1.788<br>15.620 |
| 6 | 243.1 | 349.6 | 1.540<br>4.495<br>7.582 | 232.6 | 334.5 | 7.570<br>6.104<br>2.645 |
| 7 | 298.9 | 429.8 | 2.088<br>5.402<br>12.973 | 304.4 | 437.8 | 1.776<br>3.149<br>13.281 |
| 8 | 439.9 | 632.6 | 0.106<br>0.253<br>18.796 | 493.2 | 709.3 | 0.061<br>0.131<br>19.061 |

**Table S5. Wave functions with definite projection of the total moment $|m_J>$ for of the lowest Kramers doublets (KDs) of individual Dy(III) fragment model 1(Dy1A) and model 1(Dy1B) for 1R2R-ZnDy.**

| | *E* / $cm^{-1}$ | wave functions |
|---|---|---|
| **1** | 0.0 | 83.6%\|±15/2>+14.7%\|±11/2> |
| | 68.9 | 4.3%\|±11/2>+28.1%\|±9/2>+22.9%\|±7/2>+12.4%\|±5/2>+14.5%\|±3/2>+15.7%\|±1/2> |
| **2** | 0.0 | 90.0%\|±15/2>+5.8%\|±9/2> |
| | 70.9 | 10.4%\|±9/2>+26.1%\|±7/2>+19.1%\|±5/2>+19.4%\|±3/2>+18.4%\|±1/2> |

# References


1. Y. Jinag, L. Gong, X. Feng, W. Hu, W. Pan, Z. Li and A. Mi, *Tetrahedron.* 1997, **53**, 14327-14338.
2. *CrysAlisPro*. Version 1.171. 36.28; Agilent Technologies, Santa Clara, CA, 2013.
3. G. M. Sheldrick, A short history of SHELX. *Acta Crystallogr. Sect. A: Found. Crystallogr.* 2008, **64**, 112-122.
4. A. L. Spek, Single-crystal structure validation with the program PLATON. *J. Appl. Crystallogr.* 2003, **36**, 7-13.
5. L. F. Chibotaru, L. Ungur, *Ab* initio calculation of anisotropic magnetic properties of complexes. I. Unique definition of pseudospin Hamiltonians and their derivation. *J. Chem. Phys.*, 2012, **137**, 064112.
6. L. F. Chibotaru, L. Ungur, C. Aronica, H. Elmoll, G. Pilet and D. Luneau, Structure, Magnetism, and Theoretical Study of a Mixed-Valence $Co^{II}_3Co^{III}_4$ Heptanuclear Wheel: Lack of SMM Behavior despite Negative Magnetic Anisotropy, *J. Am. Chem. Soc.,* 2008, **130**, 12445-12455.
7. L. F. Chibotaru, L. Ungur and A. Soncini, The Origin of Nonmagnetic Kramers Doublets in the Ground State of Dysprosium Triangles: Evidence for a Toroidal Magnetic Moment. *Angew. Chem., Int. Ed.*, 2008, **47**, 4126-4129.
8. F. Aquilante, J. Autschbach, R. K. Carlson, L. F. Chibotaru, M. G. Delcey, L. D. Vico, I. F. Galván, N. Ferré, L. M. Frutos, L. Gagliardi, M. Garavelli, A. Giussani, C. E. Hoyer, G. Manni, L. H. Lischka, D.-X. Ma, P.-Å. Malmqvist, T. Müller, A. Nenov, M. Olivucci, T. B. Pedersen, B.-D. Peng, F. Plasser, B. Pritchard, M. Reiher, I. Rivalta, I. Schapiro, J. Segarra-Martí, M. Stenrup, D. G. Truhlar, L. Ungur, A. Valentini, S. Vancoillie, V. Veryazov, V. P. Vysotskiy, O. Weingart and F. Zapata, R. Lindh, MOLCAS 8: New Capabilities for Multiconfigurational Quantum Chemical Calculations across the Periodic Table. *J. Comput. Chem*. 2016, **37**, 506-541.
9. B. O. Roos, R. Lindh, P.-Å. Malmqvist, V. Veryazov and P.-O. Widmark, Main Group Atoms and Dimers Studied with a New Relativistic ANO Basis Set. *J. Phys. Chem. A*, 2004, **108**, 2851-2858.

10. B. O. Roos, R. Lindh, P.-Å. Malmqvist, V. Veryazov and P.-O. Widmark, New relativistic ANO basis sets for actinide atoms. *Chem. Phys. Lett.* 2005, **409**, 295-299.
11. C. Lee, W.-T. Yang and R. G. Parr, Development of the Colic Salvetti correlation-energy formula into a functional of the electron density. *Phys. Rev. B*, 1988, **37**, 785-789.
12. A. D. Becke, Density-functional thermochemistry. III. The role of exact exchange. *J. Chem. Phys.*, 1993, **98**, 5648-5652.
13. M. J. Frisch, G. W. Trucks, H. B. Schlegel, G. E. Scuseria, M. A. Robb, J. R. Cheeseman, G. Scalmani, V. Barone, B. Mennucci and A. G. Petersson, Gaussian 09 Rev. A.02, Wallingford, CT, 2009.
14. G. A. Petersson, A. Bennett, T. G. Tensfeldt, M. A. Al-Laham, W. A. Shirley and J. Mantzaris, "A complete basis set model chemistry. I. The total energies of closed-shell atoms and hydrides of the first-row atoms". *J. Chem. Phys.*, 1988, **89**, 2193-2198.